# DYNAMICAL MODELS BASED ON CLASSICAL LIMITS

Lectures by: R. C. Arnold
Argonne National Laboratory

Notes taken by: Robert Budny

The purpose of this lecture series will be to discuss attempts to explain high energy data using classical intuition augmented by Regge behavior.

## I. GENERAL FEATURES OF TWO BODY INTERACTIONS

Experiments show that, at high energies, $\frac{d\sigma}{d\cos\theta}$ has a very sharp peak near $\theta = 0^{\circ}$, a smaller peak at $\theta = 180^{\circ}$, and is very low in between. These general features do not change as s varies. We will not consider the backward peak until later since the backward peak can be obtained by generalizing forward peak results. These features will have important implication for the models we will discuss.

Partial wave analysis of the amplitude gives

$$A(s,t) = \Sigma(2\ell+1) f_{\ell}(s) P_{\ell}(\cos\theta) \tag{1.1}$$

which can be normalized so $\frac{d\sigma}{dt} = \frac{1}{4k^2}|A|^2$. Unitarity at low energies gives

$$f_{\ell}(s) = \frac{e^{2i\delta_{\ell}(s)} - 1}{2ik} \quad , \text{ where } \delta \text{ would be real.}$$

The observation that $\frac{d\sigma}{dt}$ is very small between the forward and backward peaks indicates that many partial waves contribute to (1.1) so it is plausible to replace the sum over $\ell$ with an integral. Near the forward direction and $\ell$ large, $P_{\ell}(\cos\theta) \simeq J_0(\ell\theta)$. Define $b \equiv \frac{\ell}{k}$ = the impact parameter. Since $(-t)^{\frac{1}{2}} \simeq k\theta$, (1.1) becomes

$$A = i \int_0^{\infty} b\, db J_0(b(-t)^{\frac{1}{2}}) f(s,b) \quad . \tag{1.2}$$

The integral can be extended to $\ell = 0$ since low $\ell$ waves do not appear important. If f(s,b) is approximately factorizable then the shape of the forward peak is independent of s, as is observed. In some cases the peak shrinks as s increases, but we will assume that this is not crucial.

Several aspects of (1.2) should be noted. The arguments used to motivate it from (1.1) are heuristic. However, (1.2) can be used as an exact representation of A in impact parameter space. In the case of spinning particles, (1.2) can be easily generalized by making b a 2 dimensional vector $\perp$ to the incident momentum (see Fig. 1). Then an integral representation for $J_0$ gives

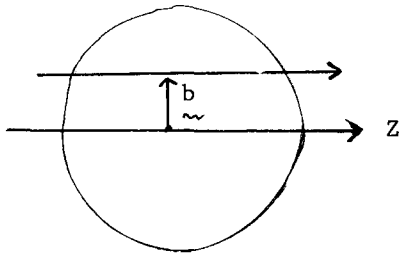


Center-of-mass System coordinates

Fig. 1

$$A(s,t) = \int d^2\underline{b}\, e^{i\underline{q}\cdot\underline{b}} F(s,\underline{b}) \tag{1.3}$$

which is the 2 dimensional Fourier transformation. For spinless particles, F depends only on s and $|\underline{b}|$. The representations (1.2) and (1.3) are very useful when s is large, t is small, and the radius of the interaction region large. In the resonance region where s is small, these representations could be used, but would be very complicated. When is large, t is approximately the transverse momentum transferred and $|\underline{q}|^2 \simeq -t$. The deBroglie wave packet spread is proportional to $\frac{1}{k}$ so at high s the wave packet feels only a small part of the scatter at a time. $b_{max}$ is of the order of the $\pi$ Compton wavelength. We might expect classical physics to be useful for constructing models when the wave packet size is much smaller than $b_{max}$.

The problem now is to find f(s,b). The concept of a potential is very useful in classical physics so let us try to use it to generate f(s,b). One aspect of this concept which will be useful to us is the additivity of potentials. Sometimes the potential of a composite system is the sum of the potentials of each constituent, e.g., nuclear scattering or the quark model. We will use potentials which are instantaneous in time and depend on spatial parameters.

Suppose we are given a potential. How can we use it? 1) Schrödinger's equation is not relativistically invariant. Since we are interested in velocities close to c, we must be cautious. 2) Covariant equations lead to retardation difficulties. 3) The last possibility is to use the potential as an effective potential, i.e., like a single scattering term. If we know the outgoing and incoming wave function, we know the scattering matrix. The equation of motion is equivalent to a definition of the potential.

Consider one dimensional motion through a slowly varying potential[1]:

$$H\psi = i\frac{\partial}{\partial t}\psi = (P^2+V)\psi, \quad P = -i\frac{\partial}{\partial x} \tag{1.4}$$

is Schrödinger's equation where $2m = \hbar = 1$. We expect the incoming wave to be modified by a phase change and absorption. The boundary condition is $\psi \to e^{-i(kx-\omega t)}$ as $x \to \infty$ so it is reasonable to try $\psi(x,t) = e^{-iW(x,t)}$. This gives

$$\frac{\partial W}{\partial t} = i\frac{\partial^2 W}{\partial x^2} + \left(\frac{\partial W}{\partial x}\right)^2 + V \quad . \tag{1.5}$$

The trial solution $W = \alpha \int_{-\infty}^{x} dx' V(x') - kx + \omega t$ where $\alpha, \omega$ are undetermined parameters gives

$$\omega = i\alpha\frac{dV}{dx} + (\alpha V(x) - k)^2 + V \quad . \tag{1.6}$$

We want to satisfy this for any V(x) so the choice $\omega = k^2$ and $\alpha = \frac{1}{2k}$ leaves

$$0 = \frac{i}{2k}\frac{dV}{dx} + \frac{1}{(2k)^2}V^2$$

where $k \gg V$, $\frac{dV}{dx}$ this is satisfied. This the eikonal approximation.

The eikonal wavefunction is

$$\psi = \exp\left[-\frac{i}{2k}\int_{-\infty}^{x} dx'V(x')+i(kx-\omega t)\right] . \tag{1.7}$$

This is essentially the WKB approximation in one dimension. In three dimensions the eikonal wavefunction is given by

$$\psi(\underline{b},x) = \exp\left[-\frac{i}{2k}\int_{-\infty}^{x} dx'V(\underline{b},x')+i(kx-\omega t)\right] \tag{1.8}$$

assuming that there is negligible transverse deflection of the incident particle, i.e., that $\theta \simeq 0$.

The transition matrix element from state $\underline{k}$ to state $\underline{k}'$ is

$$T(k',k) = i\int d^3x V(x)\psi_k^{out}(x)e^{i\underline{k}'\cdot\underline{x}} . \tag{1.9}$$

Choose a coordinate system with $\underline{k}$ along the z axis. Define $\underline{q} = (k_x'-k_x, k_y'-k_y)$. Substitute (1.7) for $\psi_k^{out}(x)$ in (1.9) and compare with (1.3). Note $k_z' \simeq k_z$ so $e^{i(k_z-k_z')z} \simeq 1$. This gives

$$F(s,\underline{b}) = \int_{-\infty}^{\infty} V(b,z)dz\ \exp\left[-\frac{i}{2k}\int_{-\infty}^{z} dz'V(\underline{b},z')\right] . \tag{1.10}$$

(See Ref. 1). The s dependence is in V(b,z). A similar result can be obtained from the Bethe-Salpeter equation. The integral in (1.10) is of the form $\int_a^b dxf'(z)e^{f(z)} = e^{f(b)}-e^{f(a)}$. Thus

$$F(s,\underline{b}) = 1-\exp\left[-\frac{i}{2k}\int_{-\infty}^{\infty} V(z,\underline{b})dz\right] \equiv 1-e^{i\chi(s,\underline{b})} \tag{1.11}$$

with

$$\chi(s,\underline{b}) = -\frac{i}{2k}\int_{-\infty}^{\infty} V(z,\underline{b})dz . \tag{1.12}$$

Note that the assumption of a straight line trajectory is essential in getting (1.11). Equations (1.11) and (1.12) constitute the eikonal approximation to the amplitude. This is comparable to the partial wave expansion (1.1) with $\chi(s,b) = 2\delta_{\ell=kb}(s)$;

$$T_{eikonal} = \int d^2\underline{b} e^{i\underline{q}\cdot\underline{b}}(1-e^{i\chi}) \quad . \tag{1.13}$$

The essence of the eikonal approximation is that the phase shift is a homogeneous linear functional of the potential (Ref. 2).

We would like to describe the eikonal approximation without using the Schrödinger equation. Defining a "Born approximation" allows us to do this. If V is small then

$$T = T_{Born} = \int d^2\underline{b} e^{i\underline{q}\cdot\underline{b}}(1-e^{i\chi}) \tag{1.14}$$

which can be inverted, since $\chi$ is small, to give

$$\chi = \int d^2\underline{q} e^{i\underline{q}\cdot\underline{b}} T_{Born}(\underline{q}) \quad . \tag{1.15}$$

(see Ref. 2)

Equation (1.15) and $F = 1-e^{i\chi}$ can be used as a starting point for the eikonal approximation. Incidently, these are true in the optical model. This allows us to use $T_{Born}$ in the sense of a relativistic single scattering term at high energies. The eikonal approximation shows how to iterate such a term to get the complete amplitude.

We need a model for $T_{Born}$ on the mass shell. Note that the connection of $\chi$ with $T_{Born}$ is trivial if we assume $\chi$ small. We extend the small $\chi$ functional form to large $\chi$. How do we know that calculating higher terms in $\chi$ (multiple scattering corrections) gives reasonable results? The approach works in molecular and nuclear physics so let's be optimistic and try. The goal is to find a $T_{Born}$ that will explain many features of data simply.

## II. SCATTERING BY COMPOSITE SYSTEMS[3-6]

Consider the scattering of an elementary particle by a composite system A. (Fig. 2) We will assume that there is an additive 2 body potential between the projectile and each constituent. We also assume no recoil or motion of the constituents during the collision. Then $V_A(b,z) = \sum_j V_j(b-b_j, z-z_j)$ where the E dependence is suppressed. The additivity of the potential implies that the phase shifts are additive so

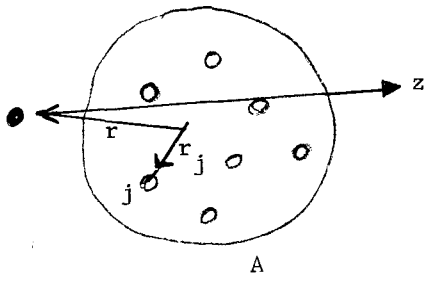


Fig. 2

$$\chi_A(\underline{b}) = \frac{i}{2k}\int_{-\infty}^{\infty} V_A(\underline{b},z)dz = \sum_j \chi_j(\underline{b}-\underline{b}_j) \quad . \tag{2.1}$$

The potential concept was used to motivate the additivity of the phase shifts.

For a quantum description of target, use nuclear wave function

$$|\psi_1(r_1 \ldots r_n)> = \text{initial state}$$
$$|\psi_2(r_1 \ldots r_n)> = \text{final state} \quad .$$

The transition amplitude is

$$T_{12} = <2|T(b,b_1 \ldots b_n)|1> = \int \psi_2^*(r_1 \ldots r_n) T(b;b_1 \ldots b_n) \psi_1(r_1 \ldots r_n) d^3r_1 \ldots d^3r_n \tag{2.2}$$

where $\underline{r}_j = (\underline{b}_j, z_j)$. For elastic scattering $\psi_1 = \psi_2$ so (2.2) becomes

$$T_{11}(b) = \int \rho(r_1 \ldots r_n) T(b;b_1 \ldots b_n) d^3r_1 \ldots d^3r_n \tag{2.3}$$

with $\rho = |\psi|^2$. The integration weighs each specific configuration with its probability.

In Glauber's theory of multiple scattering one defines "profile functions"

$$\Gamma_A \equiv 1 - e^{i\chi_A} \quad , \quad \Gamma_j \equiv 1 - e^{i\chi_j(b-b_j)}$$

which implies

$$1-\Gamma_A = \pi_j(1-\Gamma_j) \text{ or } \Gamma_A = \sum_j \Gamma_j - \sum_{\substack{i,j \\ (i\neq j)}} \Gamma_i\Gamma_j + \ldots \tag{2.4}$$

with N summations. This is a multiple scattering series. The first term is linear in scattering from each constituant and is called the impulse term since it gives the impulse approximation. The second term corresponds to two scatterings. Our approximation that the scattering is mainly forward means that the projectile is unlikely to be scattered twice by the same constituent as in Fig. 3.

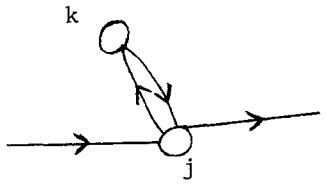


Fig. 3

As an example consider the elastic scattering of a $\pi$ on deuterium.[1]

$$T_D(b) = \int d^3r \left\{\Gamma_p(b-b_1)+\Gamma_n(b-b_2)-\Gamma_p(b-b_1)\Gamma_n(b-b_2)\right\} \rho(r)$$

$$\underline{r} = (\underline{b}_1, z) \qquad |\psi|^2 = \rho \sim e^{-\alpha^2 r^2} = e^{-\alpha^2(\underline{b}_1^2+z^2)}$$

$$\left(\frac{d\sigma}{dt}\right)_{p,n} \sim e^{t/4\beta^2} \tag{2.5}$$

assumed for scattering the $\pi$ on free protons and neutrons implies that in the eikonal approximation $\Gamma_{p,n} \sim ce^{-\beta^2 b^2}$. The single scattering terms give

$$\int d^3r \rho(r)\Gamma(b-b_1) = ce^{-(\alpha^2+\beta^2)b^2} \tag{2.6}$$

and the double scattering term gives

$$\int d^3r \rho(r)\Gamma(b-b_1)\Gamma(b+b_1) = c^2 e^{-(\alpha^2+2\beta^2)b^2} \quad . \tag{2.7}$$

The Fourier transform from impact parameter space to momentum transfer space gives

$$T(t) = ic\left\{\exp\left[\frac{t}{4(\alpha^2+\beta^2)}\right] - c\exp\left[\frac{t}{4(\alpha^2+2\beta^2)}\right]\right\} \tag{2.8}$$

$\frac{d\sigma}{dt}$ is proportional to the square of T(t) and has the features shown in Fig. 4. In general $\frac{d\sigma}{dt}$ has N slopes when there are N constituants. As $N \to \infty$ the curve becomes a Bessel function as in Fig. 5. This effect is observed in heavy nuclei.[7-9]

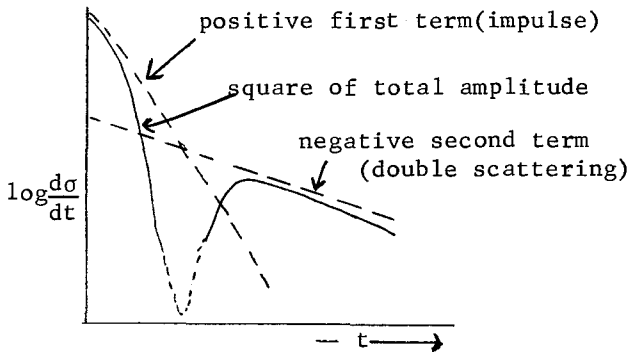


Fig. 4

Now we will relate the eikonal approximation to the droplet model[10-12] by making the number of constituents in our composite model $N \to \infty$. Assume all the constituents have the same wave function, for instance they could be in harmonic oscillator wave functions. Define S by $T(b;b_1 \ldots b_n) = 1-S(b;b_1 \ldots b_n)$. Assuming the scattering is independent gives $S = \prod_j S_j(b-b_j)$ where $S_j(x) = 1-\Gamma_j(x) = e^{i\chi_j(x)}$. Calling $\rho_j(r) = \varphi_j^*(r)\varphi_j(r)$, using the factorization properties of $\varphi$ and S, and normalizing with $< 2|1 > = 1$

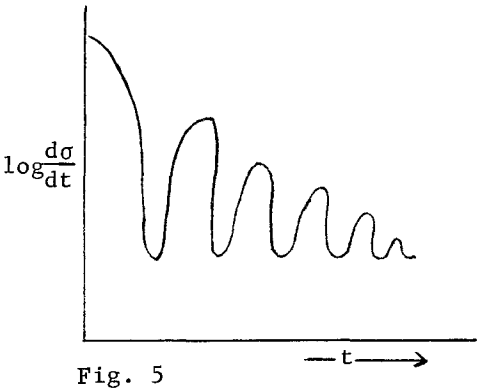


Fig. 5

in (2.2) gives

$$T(b) = 1 - \prod_{j=1}^{n} \int d^3 r_j \rho_j(r_j) e^{i\chi(b-b_j)} = 1 - \left[ S_0(b) \right]^N \tag{2.9}$$

where

$$S_0(b) = \int d^3 r \rho(r) e^{i\chi(b-b_r)} = 1 - \Gamma_0(b) \quad . \tag{2.10}$$

$\Gamma_0(b)$ is the T matrix for one constituant. Then

$$T(b) = 1 - \left[ 1 - \Gamma_0(b) \right]^N \quad . \tag{2.11}$$

We want to get a simple result as $N \to \infty$. If we hold the cross section of the composite system constant, then the cross section of each constituent must decrease. A canonical assumption is

$$\Gamma_0(b) = \frac{1}{N} \gamma(b).$$

This gives

$$T(b) = 1 - \left[ 1 - \frac{\gamma(b)}{N} \right]^N \xrightarrow[N \to \infty]{} 1 - e^{-\gamma(b)}. \tag{2.12}$$

Now consider the short range approximation. The term $e^{i\chi(b-b_1)}$ in (2.10) acts as a delta function of $b-b_r$. Define

$$D(b) = \int_{-\infty}^{\infty} \rho(b,z) dz \quad .$$

Then $\Gamma_0(b) = \frac{\gamma(0)}{N} D(b)$ gives

$$T(b) = 1 - e^{-\gamma(0) D(b)} \quad . \tag{2.13}$$

The number $\gamma(0)$ is given by experiment. D(b) is independent of the projectile in this approximation. When the projectile is complex the same result holds. As an example, in optics $\gamma(0)$ is the opacity and D(b) corresponds to the optical depth. Another example is $\pi$N scattering where D(b) has the shape given in Fig. 6. D(b) is the distribution of the proton with "R" representing its size. A third example is scattering from a nucleus.[7-9] D(b) is given by Fig. 7.

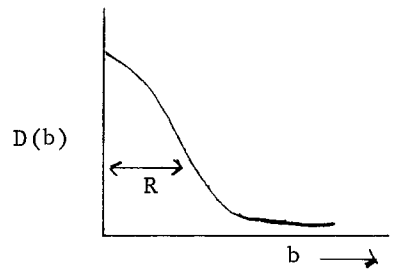


Fig. 6

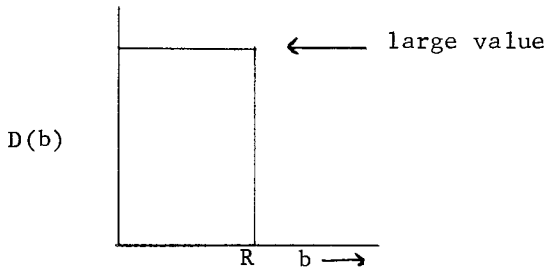


Fig. 7

$$1-e^{-\gamma(0)D(b)} = \begin{cases} 1 & b < R \\ 0 & b > R \end{cases} \tag{2.14}$$

which gives (from (1.2) and (1.11)),

$$T(t) = i\int_0^\infty bdbJ_0(b(-t)^{\frac{1}{2}})[1-e^{-\gamma(0)D(b)}]$$

$$= i\int_0^R bdbJ_0(b(-t)^{\frac{1}{2}}) = \frac{iR^2J_1(R(-t)^{\frac{1}{2}})}{R(-t)^{\frac{1}{2}}} \equiv iR^2F(t) \tag{2.15}$$

F(t) is plotted in Fig. 8. T gives the diffraction pattern of black spheres. When $\gamma$ is purely real it gives an imaginary T. $\gamma$ can be made complex to give the correct phase for (say) $\pi N$ scattering. Then (2.15) predicts T for $\pi A$ scattering where N is a nucleon and A a nucleus. Fits to high energy $\pi p$ and pp elastic scattering using as free parameters $Re\gamma$ and $Im\gamma$, and assuming[10,11] that D is given by electromagnetic form factors, agree to about 10% when $-t < 1$ GeV$^2$, as sketched in Fig. 9. In practice $Im\gamma$ can be neglected. Note

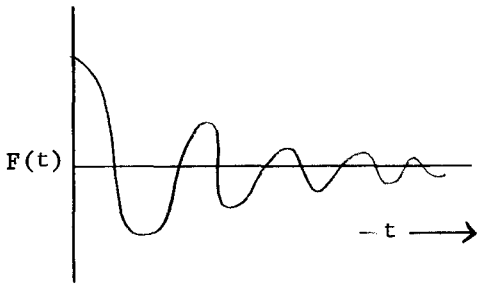

Fig. 8

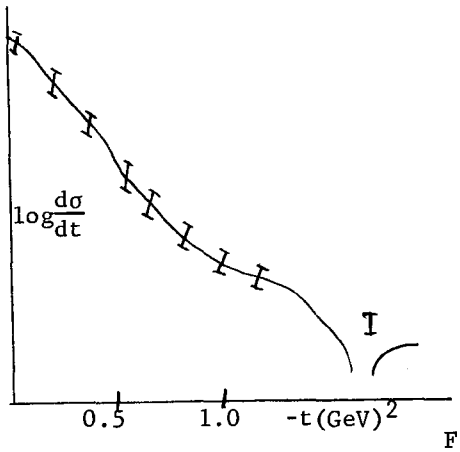

Fig. 9

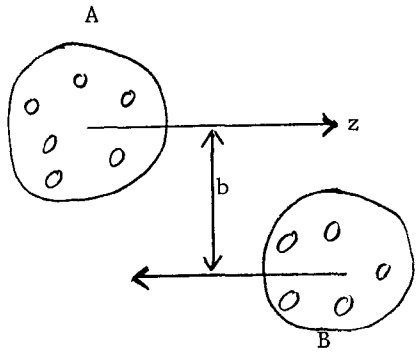

Fig. 10

that this model is inconsistent with moving Pomeron models since there is no shrinkage. The model gives $\sigma_{tot} = 2\sigma_{el} = 2R^2$, for the nuclear case (2.15).

Now we will generalize to the scattering of two composite systems A,B. See Fig. 10. The separation of the center of masses at collision is b.

$$T_\alpha(b_\alpha) = \int d^3r_1 \ldots d^3r_N \langle B,2|T(b_\alpha;b_1 \ldots b_N)|B,1\rangle , \tag{2.16}$$

where $\alpha$ is a constituent in the projectile, A. This can be summed over $\alpha$ to give

$$T_{AB}(b) = \int d^3r'_{1_A} \ldots d^3r'_{N_A} \langle A,2 \left| \left[ 1 - \prod_{\alpha} (1 - T_{\alpha}(b - b_{\alpha})) \right] \right| A,1 \rangle . \quad (2.17)$$

For elastic scattering this becomes

$$T_{AB}^{el}(b) = 1 - \prod_{\alpha=1}^{N_A} \int d^3r_1 \rho_A(r_1) e^{i\chi_B(\underline{b}-\underline{b}_{r_1})} \quad (2.18)$$

where $i\chi_B \equiv i\chi_{(\text{constituant } +B \rightarrow \text{ constituant } +B)} = -\alpha(0)D(b)$. In the short range approximation as $N_A$, $N_B \rightarrow \infty$ we find

$$T_{AB}^{el}(b) = 1 - \left[ \int d^3r'_1 \rho_A(r_1) e^{i\chi_B(\underline{b}-\underline{b}_{r_1})} \right]^{N_A} \rightarrow 1 - e^{i\chi_{AB}(b)} \quad (2.19)$$

with

$$\chi_{AB}(b) = i\gamma(0) \int d\underline{b}' D_A(\underline{b}' - \underline{b}) D_B(\underline{b}') \quad . \quad (2.20)$$

This is a convolution of the distributions. When $\gamma$ is constant this is the "coherent droplet model" of Chou and Yang.[3] The qualitative features of (2.18) and (2.19) hold even if $N \neq \infty$. $D_A(b)$ and $D_B(b)$ can be successfully (for $\pi N$ and $NN$ scattering) estimated by electromagnetic form factors. This approach can be applied to inelastic scattering with $D_A(b)$ interpretated as an operator[5] that rearranges the distribution of A. What is needed are excitation form factors, e.g., $\gamma N \rightarrow N^*$.

The qualitative features of a multiple scattering series can be seen using a Gaussian for $\chi(b) = ice^{-b^2/2R^2}$ which can be justified from Regge theory (where R depends on s), from statistical mechanics, or pragmatically. It gives

$$T(t) = iR^2 \left\{ ce^{tR^2/2} - \frac{c^2}{22!} e^{tR^2/4} + \ldots - \frac{(-c)^n}{nn!} e^{tR^2/2n} + \ldots \right\} . \quad (2.21)$$

When -t is small the series damps rapidly; however, for large -t higher order terms in the interaction strength c are important. The number of terms that are important is proportional to $|t|$. See Fig. 11. When -t is very large the saddle point from the method of least descent gives the envelope $e^{-(R(-t)^{\frac{1}{2}})}$ for T. This is the Jaffe bound.

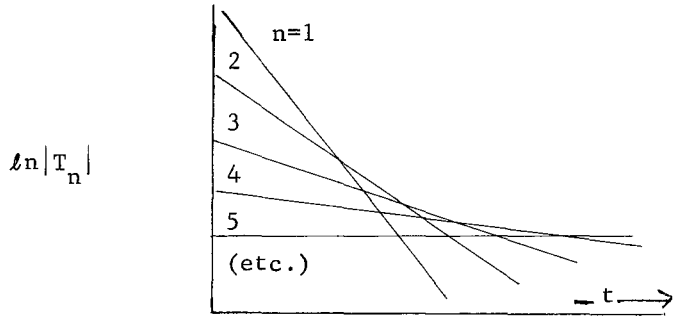


Fig. 11

## III. ABSORPTIVE FORMULA

We want to lead up to including Regge poles. Suppose $V_{effective} = V_0+V_1$ where $V_1$ is weak and $V_0$ has a simple or known form. For instance $V_0$ could come from the Pomeron and $V_1$ from the charge exchange or isospin dependent part. We have $\chi(b) = \chi_0(b)+\chi_1(b)$ where $\chi_1 \ll 1$ for all important b. In charge exchange this is satisfied when the energy is sufficiently high. Then

$$T(b) = 1-e^{i\chi} \simeq 1-e^{i\chi_0}(1+i\chi_1)=(1-e^{i\chi_0})-ie^{i\chi_0}\chi_1 \quad . \tag{3.1}$$

Following (1.2) and (1.11), define

$$T_0(t) = i\int bdbJ_0(b-(-t)^{\frac{1}{2}})[1-e^{i\chi_0(b)}] \tag{3.2}$$

$$T_1(t) = T-T_0= \int bdbJ_0(b(-t)^{\frac{1}{2}})e^{i\chi_0(b)}\chi_1(b) \quad . \tag{3.3}$$

Equations (3.2) and (3.3) are known as the absorption formula, also called the Sopkovich-Jackson-Gottfried absorption formula, or the distorted wave Born approximation because the factor $e^{i\chi_0(b)}$ distorts the usual Born formula. If $T_0(t)$ is known from the high energy limit of data, then we can invert $T_0(b)$ to get $e^{i\chi_0(b)}$. The data on $T_1(t)$ gives $\chi_1(b)$ since $T_1(t)$ is linear in $\chi_1(b)$.

As an illustration consider the black disk approximation in a nucleus. Figure 12 shows an example of what can occur in impact parameter space. $T_1(t)$ has the lower partial waves absorbed by the $e^{i\chi_0(b)}$ factor. Figure 13 shows what this gives in t space. The $J_0$ and $J_1$ contributions are out of phase. This phenomena is clearly seen in nuclei.

We could get $\chi_1(b)$ from one particle exchange with amplitude $\frac{g^2}{\mu^2-t}$. It is known that the absorption formulas describe modifications due to elastic scattering in the initial and final states. See Fig. 14. The formalism discussed above applied to inelastic processes like $\pi^o p \to \pi^+ n$. We would like to extend it to processes like $\pi^- p \to \omega n$ which is not really charge exchange unless we invoke SU(6) to equate the $\pi$ and $\omega$. This is not totally satisfactory. Another

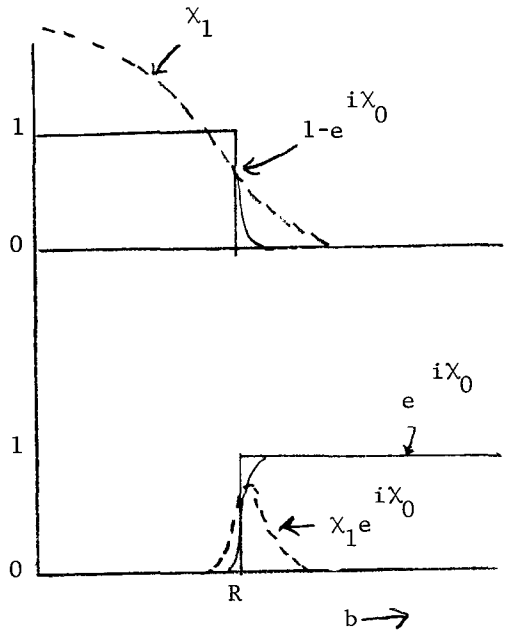


Fig. 12

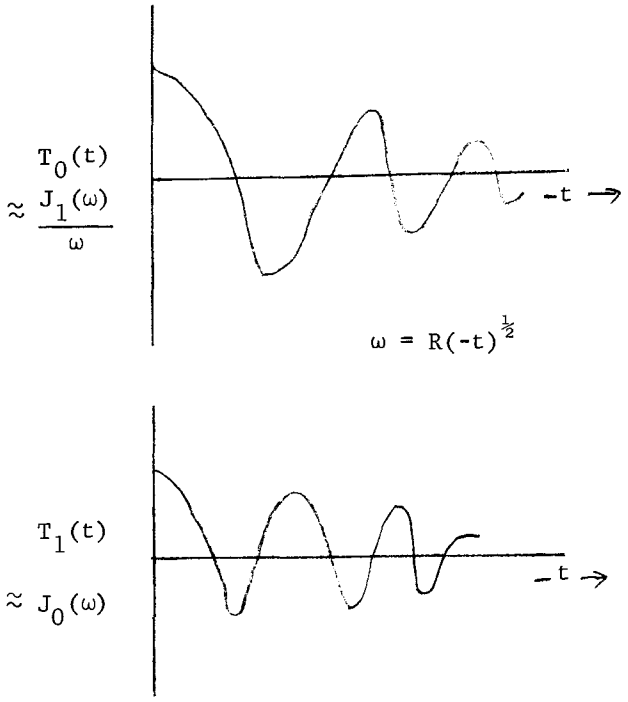


Fig. 13

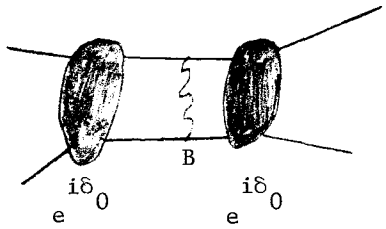


Fig. 14

justification of the application of the formalism to this reaction comes from studying the multichannel version of the problem.[2] Let channel 1 be $\pi p$ and channel 2 be $\omega n$. Then we can associate different potentials for different channels.

$$T_{11}(\pi p \rightarrow \pi p): V_{11}$$
$$T_{22}(\omega n \rightarrow \omega n): V_{22}$$
$$T_{12}(\pi p \rightarrow \omega n): V_{12} \ . \qquad (3.4)$$

Then

$$T(t) = \begin{pmatrix} T_{11} & T_{12} \\ T_{21} & T_{22} \end{pmatrix} = i\int bdbJ_0(b(-t)^{\frac{1}{2}})e\left\{\underset{\sim}{I}-\exp[i\underset{\sim}{\chi}(b)]\right\} \qquad (3.5)$$

with $\underset{\sim}{\chi} = \underset{\sim}{\chi}_0+\underset{\sim}{\chi}_1$, $\underset{\sim}{\chi}_0$ diagonal and $\underset{\sim}{\chi}_1$ off diagonal, $\ll \underset{\sim}{I}$. If we ignore non-commutativity of $e^{i\underset{\sim}{\chi}_0(b)}$ and $i\underset{\sim}{\chi}_1(b)$, we get

$$\underset{\sim}{T}_1(t) = \int bdbJ_0(b(-t)^{\frac{1}{2}})e^{i\underset{\sim}{\chi}_0(b)}\underset{\sim}{\chi}_1(b) \ . \qquad (3.6)$$

Usually it is assumed that $V_{11} = V_{22}$ so $\underset{\sim}{\chi}_0 = I\chi_0$ avoids the commutation problem.

## IV. EFFECTIVE POTENTIAL AND OPTICAL MODEL

The formula

$$T(t) = i\int bdbJ_0(b(-t)^{\frac{1}{2}})[1-e^{i\chi(b)}] \tag{4.1}$$

was derived by considering the matrix element for the scattering of an elementary projectile by a composite target.

$$e^{i\chi} = <0|e^{i\sum_j \chi_j^{elem}}|0> \tag{4.2}$$

We then assumed $\chi_j^{elem}$ is independent of s and t, i.e., $gi\delta(b-b_1)$, and built up a theory of effective two body potentials for composite-composite scattering. The effective potential has a very simple constituent-constituent scattering "ancestor" even though it could appear very complicated.

So far the use of potentials was only for motivation. There are other methods of obtaining the eikonal formula. Later we will discuss a field theory with heavy vector meson exchange which gives the formula. Note that the potential description often resembles elastic unitarity so the Schrödinger equation is usually interpreted as keeping only elastic intermediate states. In composite theories rearrangements are important and are equivalent to inelasticity which in fact dominates. The nuclear optical potential in Glauber theory has much physical content in common with multiperipheral models. Unitarity gives

$$\text{Im}A = \sum \int |T_{pp \to n}|^2 d\Omega n \ .$$

In the multiperipheral model $T_{pp \to n}$ is the amplitude shown in Fig. 15. The sum over lots of intermediate states can give a Pomeron-like object, i.e., $A(s,t \simeq 0) \sim is^{\alpha(t)}$ with $\alpha(t) \simeq 1+\epsilon t$. The scattering is dominated by inelastic intermediate states.

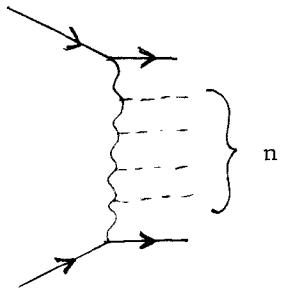


Fig. 15

In alternate models like Huang's incoherent droplet model[13] hadrons are considered arrangement of bits. Another arrangement of p gives $p+6\pi$. N depends on kinetic energy so this model is a theory of interaction, not just the states of a p alone. During a collision the bits mix randomly. To determine the probability of a final state we just count the number of rearrangements giving the state. If something like this is true,

then following Glauber, $e^{i\chi}|0>$ in (4.2) can be interpretated as a rearrangement of some of the constituants. Projecting this on $<0|$ gives the elastic matrix element, however, many inelastic intermediate states contribute. $e^{i\chi}|0>$ has a small overlap with $<0|$ for small impact parameters. In Fig. 15 the initial state has the role of $<0|$. Both approaches in their simplest versions leave out the process in Fig. 16. Later we will look at this comparison again when discussing Regge cuts.

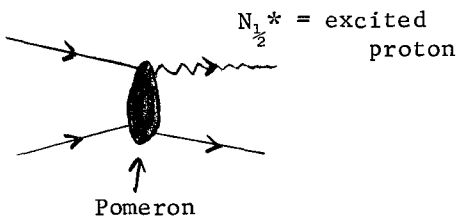


Fig. 16

Another way to study the potential is to add production processes to non-relativistic potentials.[2] This can be done with the multichannel considerations discussed previously. Denote 2-body channels by j. Then

$$(\nabla^2+k^2)\psi_1 = \sum_j V_{1j}\psi_j \tag{4.3}$$

where the momenta are assumed to be the same in each channel. In Ref. 2 it is shown that we can find an effective potential that includes multichannel effects. In general it is nonlocal. The idea of the proof is to construct Green's function for the other channels 2,..,n resulting in

$$V^{eff}(x',x) = \sum_{m,n} V_{1m}(x')G_{m\to n}(x',x)V_{n1}(x)+V_{11}(x)\delta(x'-x) \tag{4.4}$$

such that

$$(\nabla^2+k^2)\psi_1 = \int V^{eff}(x',x)\psi_1(x')dx' \ . \tag{4.5}$$

As the energy increases, we hope that (4.5) approaches $V(x)^{\text{effective-local}}\psi_1(x)$.

Recently there has been much interest in field theoretic approaches to the eikonal model.[14-20] The goal is to derive $\chi$ from a model field theory where $S=\exp i(\chi)$ and $\chi$ is the Born approximation. The most ambitious attempt is that of H. Cheng and T.T. Wu[18] in electromagnetism. Torgerson's approach[14] is to start with the interaction Lagrangian $L_{int} = g\psi\gamma^\mu\psi V_\mu$ to couple spin $\frac{1}{2}$ to neutral spin 1 particles. Elastic scattering of two fermions is then

$$<\text{final}|S|\text{initial}> = <f|T\exp\int d^4x L_{int}|i> \tag{4.6}$$

which cannot be solved in general. We want the high s limit which supposedly is a classical limit so we neglect self energy diagrams (the fermion sees only its local region). Then the only diagrams remaining are those where each vector is emitted

and absorbed by a fermion. Glauber solved (4.6) within these assumptions in 1951, getting

$$< S > = < \exp\left[ g^2 \int \Delta(x'-x) \right] > \qquad (4.7)$$

where $\Delta$ is the Born term corresponding to one vector exchange. The assumptions imply that time ordering is not needed and that the emission and absorptions are independent.

## V. REGGE EXCHANGE

Consider a one particle exchange approximation to the amplitude, $A \simeq \frac{g^2}{\mu^2 - t}$ (See Fig. 17). In configuration space this corresponds to a Yukawa potential, i.e., in the s channel we see a potential. In the t channel this looks like a resonance or bound state which shows a peak in the cross section at its mass. Since A does not depend on $\cos\theta_t$ it is an s-wave resonance in the t channel. The Chew-Frautschi plots have many resonances. We want to include a whole family in a Born term like $\frac{g^2}{\mu^2 - t}$. To do this we use the Regge theory

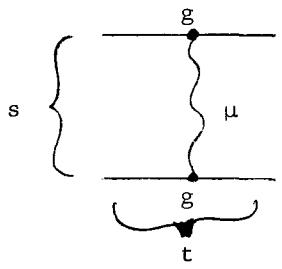


Fig. 17

formalism (ignoring signature, spin, and the possibility of cuts and fixed poles for now) to get $\beta(t)s^{\alpha(t)}$ for the amplitude at large s and fixed t. This is the Born approximation to the potential due to the exchange of the family. If $\beta(t)$ is slowly varying then we get $e^{a+bt}$ for the amplitude where $b = \tilde{b}\ell ns$ and $\tilde{b}$ = constant.

This approach gives selection rules on the particle quantum numbers. For instance, consider $\pi^- p \to \pi^0 n$. In the t channel the exchanged object must have isospin 1 so

$$\left.\frac{d\sigma}{dt}\right|_{t\simeq 0} \sim \frac{1}{s^2}\left| s^{\alpha(0)} \right|^2 = s^{2\alpha(0)-2} \quad . \qquad (5.1)$$

The relevant trajectory is that of the $\rho$ with $\alpha(0) \simeq \frac{1}{2}$. Thus the effective spin of the exchanged object is $\frac{1}{2}$. This fits the data very well whereas one particle exchange does not.

If $\alpha_P(0) = 1$ then the amount of shrinkage of $\frac{d\sigma}{dt}$ as s increases indicates the slope of the P trajectory on the Chew-Frautschi plot. Sometimes there is shrinkage and sometimes there is none, suggesting that the trajectory may be flat. This is supported by the lack of evidence for mesons on such a trajectory. These facts suggest that the Pomeron is not a Regge pole and should be treated separately. We will look for a classical description of it.

## VI. HYBRID MODEL OR ABSORPTION MODEL[21]

In this model the Pomeron singularity is assumed to come from the droplet model and to be different from ordinary Regge poles. The potential is a sum of a droplet model term and Regge terms. The droplet model implies that the Pomeron is a fixed pole. If we assume that the droplet model holds literally at positive t then it violates analyticity and unitarity. This can be rectified by a cut which masks the Pomeron pole in the $t > 0$ region of the Chew-Frautschi plot. We will not worry about this since we will apply the model only when $t < 0$. Note that we are not taking the radical Regge theory where all the singularities in the physical region of the J plane are simple moving poles. The Regge picture we will use has the following features: (not applied to elastic scattering)

1) No resonances in the t channel implies no forward peaks in the s channel (example, since no doubly charged meson resonances have been seen we expect no peaks in $\pi^+ n \to \pi^- N^{++}$ which is true experimentally).

2) The energy dependence comes from $\alpha(0)$. This we find by extrapolation from positive $m^2$.

3) Shrinkage of the forward peak in charge exchange scattering.

Competing models such as the coherent droplet model do not give the above features since they do not have crossing and thus say nothing about the t channel. The hybrid model gives the above features.

As an example of a hybrid model calculation consider $pp \to pp$ and neglect spin (which is a few percent correction). Suppose there is a Pomeron contribution to the amplitude $A_P$ and a Regge pole contribution $A_R$. Assume that

$$A_P = iC[F_p(t)]^2 \tag{6.1}$$

where $F_p$ is the electromagnetic form factor of the proton. Any non-magnetic form factor works. A useful fit is

$$F_p(t) \simeq \left(\frac{\mu^2}{\mu^2 - t}\right)^2 \tag{6.2}$$

with $\mu^2 \simeq 0.7\ \text{GeV}^2$.

(6.1) can be motivated by arguing that the interaction between bits is pointlike and the the distribution of bits is proportional to the electromagnetic form factors. We have normalized the amplitude to give

$$\frac{d\sigma}{dt} = |A(s,t)|^2 \ . \tag{6.3}$$

We next assume exchange degeneracy so

$$A_R = \beta(t) s^{\alpha(t)-1} \tag{6.4}$$

which for $[\omega+f_0,\ \rho+A_2]$ trajectories is real. For small t

$$A_R \simeq \gamma \exp(a+b_1 t)$$
$$\beta(t) \simeq \gamma \exp(b_2 t), \quad b_1 = b_2+\alpha'\ell ns, \quad \gamma = \beta(0), \quad a = [\alpha(0)-1]\ell ns. \tag{6.5}$$

We neglect one particle exchange, such as $\pi$ exchange which contributes a fraction of a millibarn when s is above 5 GeV. Equations (6.1), (6.2) and (6.5) give the eikonal

$$\chi(b) = icb^3 K_3(\mu b) + \gamma s^{\alpha(0)-1} e^{-b^2/2R^2}$$
$$= \chi_0(b)+\chi_1(b) \tag{6.6}$$

where $\chi_0$ is the Pomeron eikonal, $\chi_1$ is the Regge eikonal, $K_3$ is the third order Bessel function of imaginary argument, b is the impact parameter, and $R^2 = 2b_1$. Since $\chi_0 \gg \chi_1$ we can substitute $\chi_0$ and $\chi_1$ in (3.2) and (3.3) getting

$$T_0 = i\int b\ db\ J_0(b(-t)^{\frac{1}{2}})\left[1-e^{-cb^3 K_3(\mu b)}\right] \tag{6.7}$$

$$T_1 = \int b\ db\ J_0(b(-t)^{\frac{1}{2}})\gamma s^{\alpha(0)-1} e^{-b^2/2R^2} e^{i\chi_0(b)} \tag{6.8}$$

$e^{i\chi_0}$ can be approximated by $[1-ce^{-b^2/2R_0^2}]$. From (6.7) $|T_0|^2$ has the shape in Fig. 18 and $T_1$ becomes to second order in $b/R_0$

$$T_1 \simeq \gamma s^{\alpha(0)-1} \int b\ db J_0(b(-t)^{\frac{1}{2}}) e^{-b^2/2R^2}[1-ce^{-b^2/2R_0^2}]$$
$$\simeq \gamma s^{\alpha(0)-1}\left\{ e^{\frac{R^2 t}{2}} - c\left(\frac{R_0^2}{R_0^2+R^2}\right) e^{R_2^2 t/2}\right\} \tag{6.9}$$

with $R_2^{-2} = R_0^{-2}+R^{-2}$. $|T_1|^2$ also looks like Fig. 18 except the dips are displaced since the Pomeron and Regge pole contributions (6.1) and (6.4) are out of phase. $|T|^2$ has the shape given in Fig. 19. As s increases the Regge pole vanishes and $|T|^2 \to |T_0|^2$, i.e., the dips get deeper. We shall later study the J plane singularities which lead to the two terms in (6.9)

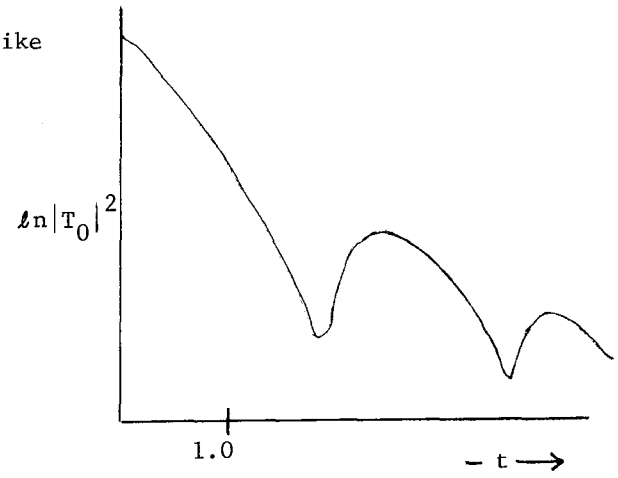


Fig. 18

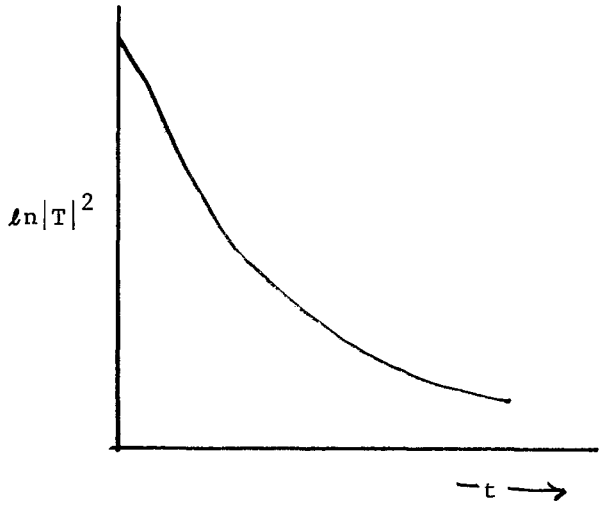


Fig. 19

## VII. COMPARISON OF MODELS

The hybrid model resulted from the assumption

$$A^{\text{Born}}(s,t) = A^{\text{droplet model}} + A^{\text{Regge pole}} \tag{7.1}$$

where $A^{\text{droplet model}}$ is due to a fixed pole at $\alpha = 1$. The Frautschi and Margolis[22-24] model used (7.1) replacing the droplet term with a moving Pomeron term. Their Pomeron is assumed to have a trajectory $\alpha(t) = 1+\alpha' t$ and phase $[1+e^{-i\pi\alpha}](\sin\pi\alpha)^{-1}$, thus they get elastic shrinkage. It is easy to pass from one model to the other if $\alpha' \simeq 0$.

Next we will compare predictions of various models for pp, $\bar{p}p$, pn scattering. $\frac{d\sigma}{dt}$ for pp and $\bar{p}p$ is given in Fig. 20. It is important to note that the curves cross over. The pp curve shrinks as s increases, the $\bar{p}p$ forward peak expands, and the dip in the $\bar{p}p$ curve becomes less pronounced. First consider what simple Regge theory implies about the cross-over. The Regge contribution to the elastic scattering is given by

$$pp = P+\omega+f_0+\rho+A_2 \tag{7.3a}$$

$$\bar{p}p = P-\omega+f_0-\rho+A_2 \tag{7.3b}$$

$$pn = P+\omega+f_0-\rho-A_2 \quad . \tag{7.3c}$$

The sign change from (7.3a) to (7.3b) is due to odd signature vector poles. The sign change from (7.3a) to (7.3c) is due to I=1 poles.

Assume the same trajectory function $\alpha(t) = \frac{1}{2}+\alpha t$ for all but P. Empirically $\sigma_{tot}(\bar{p}p) > \sigma_{tot}(pp) \simeq \sigma_{tot}(pn) \simeq$ constant for $3 < s < 20$ GeV$^2$. The optical theorem

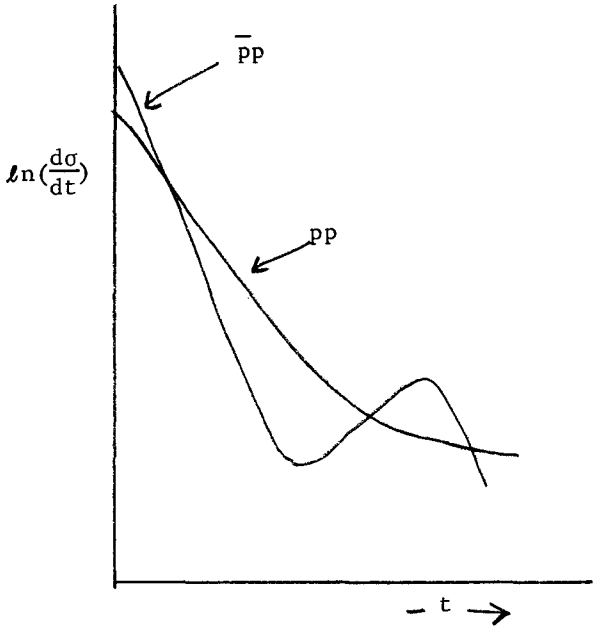


Fig. 20

then implies that $Im(\rho+A_2) = Im(-\rho-A_2)$ independent of s. Since

$$\rho = \frac{1-e^{-i\pi\alpha}}{\sin\pi\alpha} \beta_\rho(t) s^{\alpha(t)}$$

$$A_2 = \frac{1+e^{-i\pi\alpha}}{\sin\pi\alpha} \beta_{A_2}(t) s^{\alpha(t)} , \qquad (7.4)$$

if $\beta_\rho = \beta_{A_2}$ then, by (7.4), $Im(\rho+A_2) = 0$. If $\beta_\omega = \beta_{f_0}$ also then there is cancellation of $Im\omega$ with $Imf_0$ leaving only ImP in $\sigma_{tot}(pp)$ and $\sigma_{tot}(pn)$. We will assume complete exchange degeneracy $\beta_\rho(t) = \beta_{A_2}(t)$, $\beta_\omega(t) = \beta_{f_0}(t)$. This is predicted by bootstrap schemes and finite energy sum rule.

$\beta_{A_2}(t)$ requires a zero at $\alpha(t_0) = 0$ to cancel a pole in the physical region of $\pi^- p \to \eta n$. Exchange degeneracy implies that $\beta_\rho(t_0) = 0$ so $\frac{d\sigma}{dt}(\pi^- p \to \pi^0 n)$ should be 0 at $t = t_0$. This is not seen, but we can salvage exchange degeneracy by using cuts to fill in the dip at $t=t_0$. In general, to kill ghosts (as in $A_2$) and to decouple spin flip amplitudes at nonsense wrong signature points we need zeroes of $\beta$ at $\alpha = 0,-1,-2,\ldots$ corresponding to $t = -0.5$, $-1.5$, etc.[25-27]

The cross-over effect in Fig. 20 is not due to nonsense zeroes and not due to large spin flip cancellation so it remains a mystery in the simple Regge model. The hybrid model gives it nicely since cancellation of the two terms in (6.9) for some $t_0$ will give $T_1 \simeq 0$. The P term in (7.3a and b) is large and imaginary whereas the

$\rho$, $A_2$ terms are small. The $f_0$ term has the same sign for pp and $\bar{p}p$ scattering. The $\omega$ term can explain the cross-over if its contribution (plus correction) is positive for $t_0 < t < 0$ and negative for $t < t_0$.

In general from fits to polarization data we find that I=1 exchange corresponds to helicity-flip and I=0 corresponds to non-flip. The absorptive corrections to helicity-flip amplitudes are smaller than to helicity non-flip for small t.

The amplitude for the reaction $\pi^- p \to \pi^0 n$ is predominantly helicity flip. The corrections go like $t\ell ns$. The differential cross section and polarization are given by

$$\frac{d\sigma}{dt} = |G_+|^2+|G_-|^2; \quad \mathcal{P} = \frac{2\mathrm{Im}G_+^*G_-}{|G_+|^2+|G_-|^2} \tag{7.5}$$

where $G_-$ ($G_+$) is the helicity (non) flip amplitude. If the phase of $G_+$ and $G_-$ are equal then $\mathcal{P} = 0$. This is the case if only one Regge pole contributes. The simple Regge model predicts that since only $\rho$ is exchanged, $\mathcal{P}$ should be 0. Experiments give $\mathcal{P} \simeq (15\pm5\%)$ for $-t\epsilon[0.1, 0.2]\mathrm{GeV}^2$. In the hybrid model the phases of $G_+$ and $G_-$ are modified by absorptive corrections. When parameters are fitted to other reactions, the model gives Fig. 21. The ummeasured part of the polarization curve is very difficult to measure.

The polarization of the reaction $\pi^+ p \to K^+\Sigma^+$ is easier to measure since the decay of the $\Sigma^+$ indicates its polarization.[28] The relevant trajectories are the K*'s. If we assume exchange degeneracy and SU(3) symmetry we can use $\rho$ and $A_2$ parameters. The differential cross section and the calculated (M. Blackmon, private communication) and measured polarization are sketched in Fig. 22. (see next page) The break in $\frac{d\sigma}{dt}$ occurs near the point where $\mathcal{P}$ is maximum as can be seen from (7.5). Again exchange degeneracy without absorption corrections predicts zero polarization.

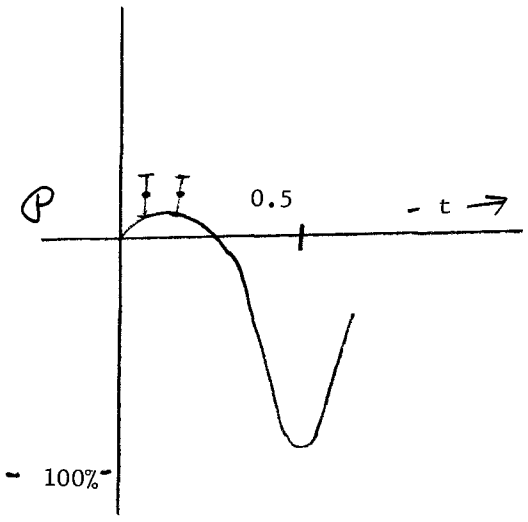


Fig. 21

Now we will study the J plane singularities corresponding to the two terms in (6.9). Recall that the Sommerfeld-Watson transformation of the partial wave series $\sum_\ell F_\ell(t)P_\ell(z_t)$ results in a background integral, a sum over Regge poles, and possibly a sum over cuts. The contour which initially enclosed the positive

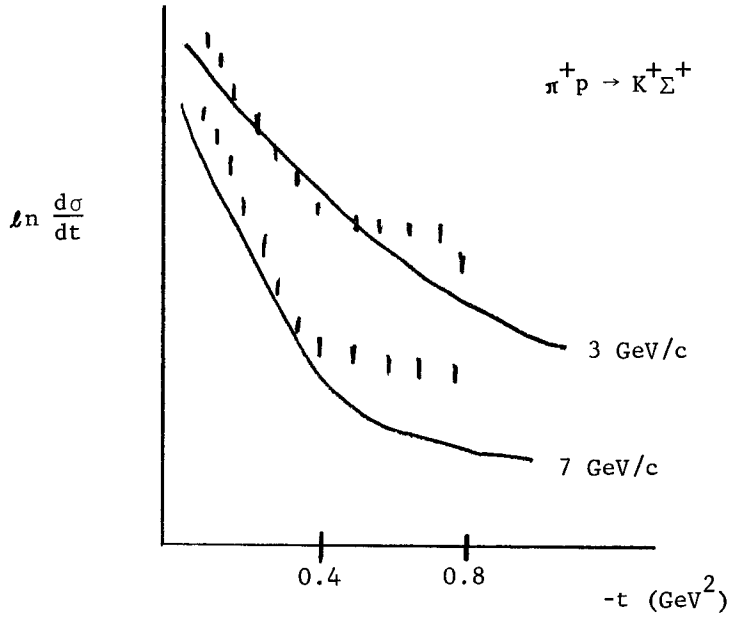
$\pi^+ p \rightarrow K^+\Sigma^+$
$\ell n \frac{d\sigma}{dt}$
3 GeV/c
7 GeV/c
0.4
0.8
$-t\ (GeV^2)$

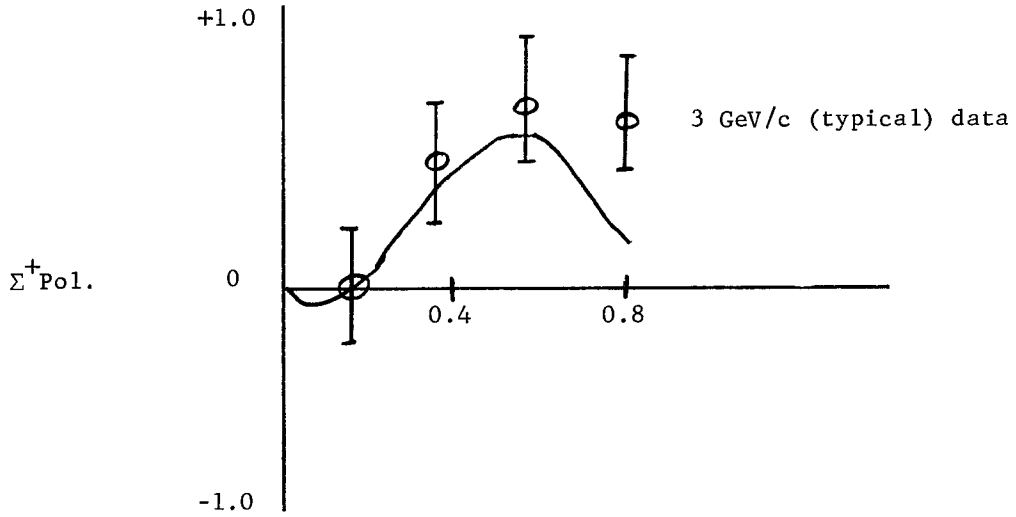
+1.0
$\Sigma^+$Pol.
0
-1.0
0.4
0.8
3 GeV/c (typical) data

Fig. 22

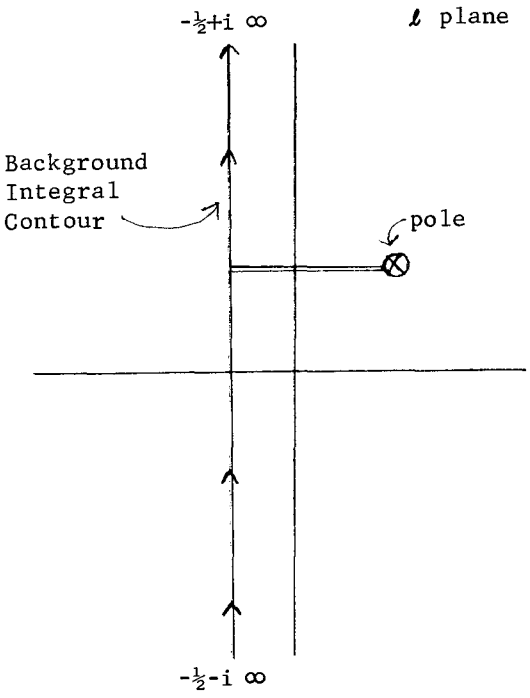


Fig. 23

integers has been opened as shown in Fig. 23. A simple pole at $\ell = \alpha(t)$ has the asymptotic behavior in s with t fixed so $\beta(t)s^{\alpha(t)}$. A cut may be represented by a dense set of poles. Asymptotically this gives

$$\int_{-\infty}^{\alpha_c(t)} W(\ell,t)s^{\ell}d\ell \quad , \tag{7.6}$$

where $\alpha_c(t)$ is the branch point and $W(\ell,t)$ is the discontinuity across the cut which has been chosen to lie left of $\alpha_c(t)$. This can be approximated by $\sum_n \beta_n(t)s^{\alpha_n(t)}$. The region of the cut away from $\alpha_c(t)$ does not effect the asymptotic behavior so only the discontinuity close to the end point matters. If the discontinuity is regular at the branch point, we may expand W

$$\begin{aligned} W(\ell,t) &= W(\alpha_c(t))+(\ell-\alpha_c(t))\left(\frac{\partial W}{\partial \ell}\right)_{\ell=\alpha_c} +..... \\ &= \beta_0(t)+(\ell-\alpha_c(t)\beta_1(t)+ .... \end{aligned} \tag{7.7}$$

and substitute in (7.6). Using $s^{\alpha} = e^{\alpha \ell n s}$, this gives

$$A = \int W(\ell,t)s^{\ell}d\ell = \beta_0(t)\,\frac{s^{\alpha_c(t)}}{\ell n s} + \beta_1(t)\frac{s^{\alpha_c(t)}}{(\ell n s)^2} +... \tag{7.8}$$

which is normalized so $\frac{d\sigma}{dt} = \frac{1}{s^2}|A|^2$. The series (7.8) converges too slowly for present experimental energies. However, if we knew the asymptotic behavior of the amplitude sufficiently well we could deduce the nature of the J plane singularities. The first term represents a constant discontinuity W. The other terms represent discontinuities that vanish at the branch point. If the Pomeron is a simple cut with constant discontinuity, then it produces a total cross section

$$\sigma_T = \frac{1}{s}\,\mathrm{Im}A(s,0) = \frac{1}{s}\,\frac{s^{\alpha_c(0)}}{\ell n s} \quad . \tag{7.9}$$

To compare with the hybrid model, consider the case $T = T_0^{\text{Pomeranchon}} +$

$T_1$ charge exchange (CEX) at t=0. Then (6.9) gives

$$T_1^{CEX}(s,0) = \left(1 - \frac{cR_0^2}{R_0^2+R^2}\right)\beta(0)s^{\alpha(0)-1}. \qquad (7.10)$$

The first term represents an ordinary Regge pole; however, since $R^2 = 2(b_2+\alpha'\ell ns)$ and $R_0$ is independent of s, the second term, which is a correction term, has the asymptotic form $\beta(0)(\ell ns)^{-1}s^{\alpha(0)-1}$ and thus represents a cut. [The normalizations in (6.9) and (7.8) differ by a factor of so the branch point and Regge pole occur at $\alpha(0)$.] As $S \to \infty$, $R^2 \to \infty$, $R_1^2 \to R_0^2 =$ constant. So for $t \neq 0$,

$$A(s,t) \to -\frac{cR_0^2}{\alpha'\ell ns} e^{tR_0^2/2}\beta(0)s^{\alpha(0)-1} \qquad (7.11)$$

where $|t\ell ns| \gg 1$ and $|\ell ns| \gg 1$. Since the power of s does not vary with t in this limit, the cut is fixed as shown in Fig. 24 for the case of the $\rho$ trajectory.

In the Frautschi-Margolis model[22-24] with a moving Pomeron, the approximation $e^{i\chi_0} \simeq 1\text{-}ce^{-b^2/2R_0^2}$ which was used to derive (6.9) must be replaced by a series of Gaussians, giving at large (-t)

$$\sum \frac{(-c)^n}{nn!} e^{tR_0^2/n} \to e^{-R_0(t)^{\frac{1}{2}}}, \qquad (7.12)$$

with $R_0^2 \propto \ell ns$. The moving cuts accumulate to an effective line as shown in Fig. 25.

Most Regge theorists believe that there are cuts[29-31] in the J plane on the evidence from perturbation theory. The first such evidence came from Amati, Fubini and Stanghellini (AFS) who studied the unitarity diagrams in Fig. 26 and found that they give a cut whose discontinuity is $\int A_n^* A_n$. Mandelstam showed that when Fig. 26 is interpreted as a Feynman diagram, off-mass-shell contributions cancel the cut. He then found non-planar Feynman diagrams such as Fig. 27, which produced cuts at the same location as the AFS cuts. Unitarity cannot be used to give the discontinuity so the importance of the diagram is unknown. The absorptive model gives the cuts in the right position and gives the discontinuity with the correct sign relative to the pole. The correct sign is important since it produces the dip, the cross-over effect, and the polarization. Other models such as that of AFS give the wrong sign. This suggests that the cut is not due to two body unitarity. The multiperipheral model also gives the wrong sign unless absorption is added in the intermediate states[32] as illustrated in Fig. 28.

If the absorptive model is correct then it contains non-planar diagrams as in Fig. 27. For example, in deuteron-deuteron scattering the diagram in Fig. 29 gives a Regge cut according to Mandelstam's argument. It is also the second term in

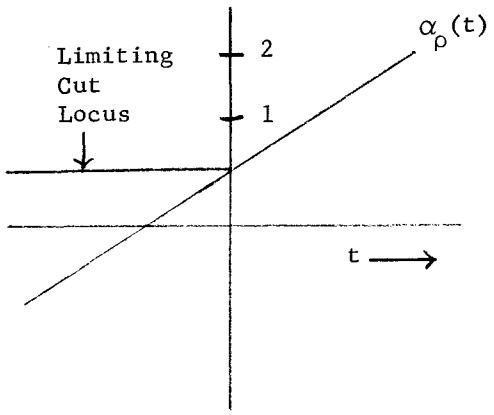


Fig. 24

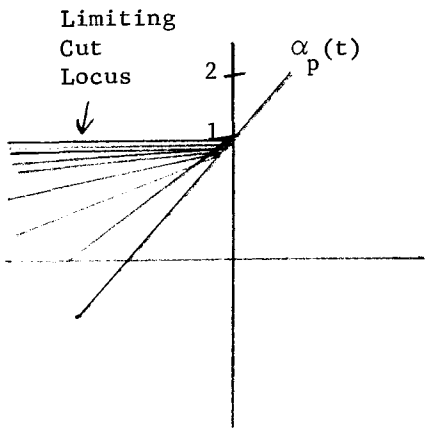


Fig. 25

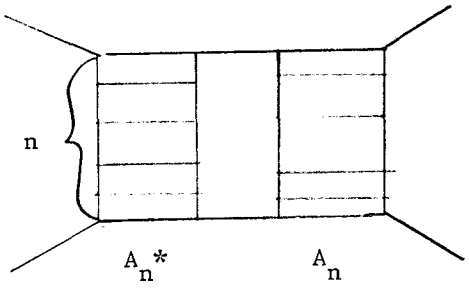


Fig. 26

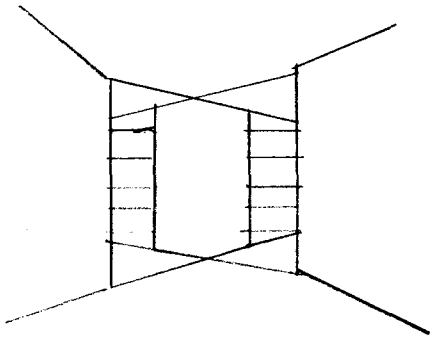

Fig. 27

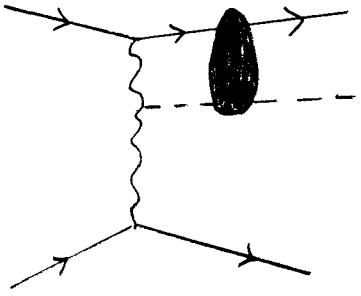

Fig. 28

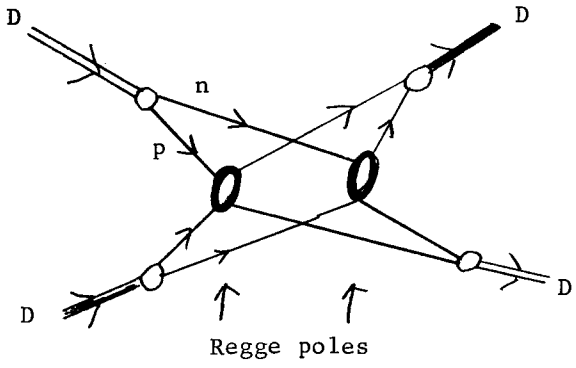


Fig. 29

the multiple scattering series.

Now we will examine in more detail the similarities and contrasts between the absorption model and unitarity models. We will see that (3.3) resembles elastic unitarity. Define $\chi_1 = A_1^{pole}(s,b)$ and $e^{i\chi_0} = 1+iA_0(s,b)$. Then (3.2) and (3.3) become

$$T_0(s,t) = \int b\, db J_0(b(-t)^{\frac{1}{2}})A_0(s,b) \tag{7.13}$$

$$T_1(s,t) = \int b\, db J_0(b(-t)^{\frac{1}{2}})[1+iA_0(s,b)]A_1^{pole}(s,b)$$

$$\equiv A_1^{pole}(s,t)+A_1^{c}(s,t) \tag{7.14}$$

where

$$A_1^{pole}(s,t) = \int b\, db J_0(b(-t)^{\frac{1}{2}})A_1^{pole}(s,b) \tag{7.15}$$

and

$$A_1^{c}(s,t) = i\int b\, db J_0(b(-t)^{\frac{1}{2}})A_0(s,b)A_1^{pole}(s,b) \tag{7.16}$$

is a correction term due to a cut. If the elastic contribution $A_0$ is mostly positive imaginary, then $A_1^{c}(s,t)$ has a minus sign relative to $A_1^{pole}(s,t)$.

The integral $\int db$ was motivated by a discrete sum on $\ell$. In the s channel $A_1^{c}$ has the expansion

$$A_1^{c} = i(\ldots)\sum_{\ell}(2\ell+1)A_{0;\ell}(s)A_{1;\ell}^{pole}(s)P_\ell(z_s) \tag{7.17}$$

where

$$A_{0;\ell}(s) = \int dz' A_0(s,z')P_\ell(z') \tag{7.18}$$

and

$$A_{1;\ell}^{pole} = \int dz'' A_1^{pole}(s,z'')P_\ell(z'') \ . \tag{7.19}$$

Then (7.16) is

$$A_1^{c} = i\int dz'dz'' A_0(s,z')A_1^{pole}(s,z'')\left[\sum_{\ell=0}^{\infty}(2\ell+1)P_\ell(z)P_\ell(z')P_\ell(z'')\right] . \tag{7.20}$$

The term in brackets is the Mandelstam kernel $\theta(\Delta)/(\Delta)^{\frac{1}{2}}$ where $\Delta = z^2+z'^2+z''^2-zz'-zz'z''-zz''+1$ and $\theta$ is the step function. In t space (7.20) becomes

$$A_1^{c}(s,t) = i\int dt'dt'' A_0(s,t')A_1^{pole}(s,t'')K(s,t;t';t'') \tag{7.21}$$

which is the absorption or eikonal formula. The Mandelstam kernel K depends on s

since the Jacobian transforming (7.20) to (7.21) does.

Now compare (7.21) with the results of two particle unitary applied to the box diagram in Fig. 30. Let B be its amplitude

$$B(s) = \int \frac{\mathrm{Im}B(s')}{s'-s}\, ds' \quad . \qquad (7.22)$$

Two particle unitarity (AFS) gives the absorptive part of B,

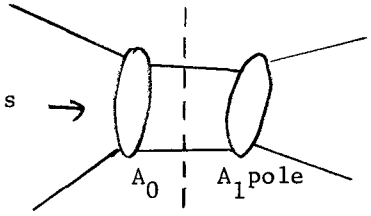


Fig. 30

$$\mathrm{Abs}[B(s)] = \int dt'dt'' A_0^*(s,t') A_1(s,t'') K(s,t;t';t'') \qquad (7.23)$$

which looks similar to (7.21). K is the same, however (7.21) is the whole amplitude unlike Abs[B]. Also, (7.23) has a complex conjugation of an amplitude which is mostly imaginary so the sign is opposite.

In (7.23) $A_1^{\text{pole}}$ is not necessarily a Regge pole. However, in such a case, suppose $A_0 \sim s^{\alpha_0(t)-1}$ and $A_1 \sim s^{\alpha_1(t)-1}$. Now K has the property that as $s \to \infty$, it is significant only when $(-t'')^{\frac{1}{2}} + (-t')^{\frac{1}{2}} \leq (-t)^{\frac{1}{2}}$. Then

$$A^c(s,t) \to \int dt'dt'' s^{\alpha_0(t')+\alpha_1(t'')-2} \quad . \qquad (7.24)$$

For large s and small t this gives

$$A^c(s,0) \sim \frac{s^{\alpha_c(0)-1}}{\ell n s} \qquad (7.25)$$

where $\alpha_c(0) = \alpha_0(0)+\alpha_1(0)-1$. The cut has the same position as the AFS model gave although the sign and magnitude are different. If we take $t \neq 0$, the slope of $\alpha_c(t)$ can be found. For instance, if we start with $\alpha_0 = \alpha_1 = \alpha_\rho$, then we get $\alpha_c' \equiv \alpha_\rho'/2$. We can iterate choosing $\alpha_0 = \alpha_{\rho\rho}$ and $\alpha_1 = \alpha_\rho$. The results are shown in Fig. 31. The cuts are not very interesting for $t > 0$ since the pole contribution dominates. If the Pomeron and $\rho$ are iterated then we get Fig. 32.

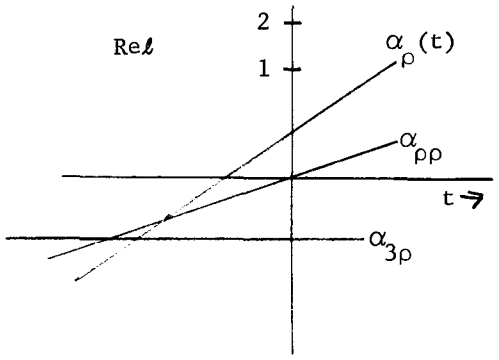


Fig. 31

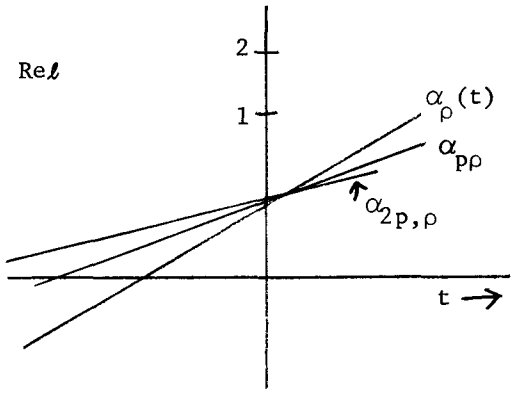


Fig. 32

To see how important the cuts are consider typical cross sections at $E \sim 20$ GeV.

$$\sigma_{total} \simeq 25 \text{ mbarns}$$

$$\sigma_{elastic} \simeq 10 \text{ mbarns}$$

$$\sigma_{charge\ exchange} \simeq 100\ \mu\text{barns (single } \rho \text{ cut)}$$

$$\sigma_{y\text{-exchange}} \simeq 70\ \mu\text{barns}$$

$$\sigma_{double\ charge\ exchange} \simeq 1\ \mu\text{barns (double } \rho \text{ cut).}$$

The last is known to be small for some reactions but could be important for the diagram in Fig. 33.

We have seen that $A_1^c(s,t)$ is related to Feynman diagrams in the shape of a box instead of unitarity diagrams such as Fig. 30. Mandelstam showed[29] that unless the intermediate particles are held on the mass shell, the Feynman diagram gives no cut. For some mysterious reason we need to throw away the contributions when the particles are off the mass shell. A heuristic justification for this is that if the intermediate particles are composite and loosely bound, then they can break up when they are off the mass shell. If we assume that the propagators oscillate wildly off the mass shell, then we need consider only mass shell contributions. Gribov and Migdal claim that the absorptive part of an amplitude such as in Fig. 26 is less than or equal to the sum over all orders of the non-planar Feynman diagrams in Fig. 34. If their argument can be strengthened then it will provide the justification.

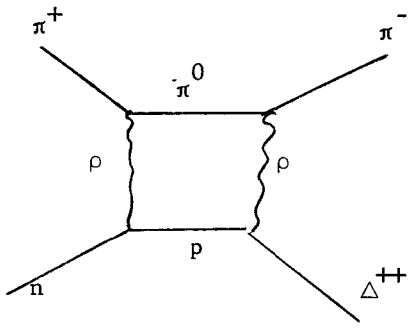


Fig. 33

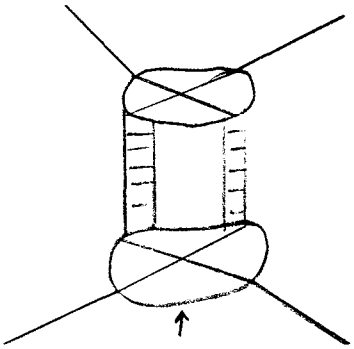

(all crossed graphs)

Fig. 34

It was pointed out earlier that the hybrid model and multiperipheral model neglect Fig. 16. It was hoped that this correction is small. The correction to the cross section has been estimated at about 10%. Henyey et. al.[33] try to make the correction by multiplying $A_1^c$ by $\lambda$ with $\lambda \geq 1$. $\lambda$ should be close to 1 since $\lambda = 1$ gave reasonable results for the cross-over effect, polarization, and $\frac{d\sigma}{dt}$. If $\lambda \gg 1$ then exchange degeneracy is intolerable and the location of dips in $\frac{d\sigma}{dt}$ depend on s.

Henyey et. al.[33] choose $\lambda \approx 2$ and get secondary peaks in $\frac{d\sigma}{dt}$ from multiple scattering. Data at higher s may decide which version of the absorptive model is better.

Another way of including absorption is to insert Regge poles in K matrix which is defined by $T = B(1-i\rho k)^{-1}$. B is the Born approximation and has resonance poles. Poles and cuts are generated by this method; however, more art is needed to explain data.

## VIII. THEORIES OF PRODUCTION

A simple but unsuccessful model for production is the bremsstrahlung model which results from assuming that the particles are produced by the legs of elastic scattering amplitudes as illustrated in Fig. 35. The amplitude for the diagram is $A_e(s,t)\frac{g}{s_1-m^2}$ with $A_{e\ell}$ assumed to be the mass-shell amplitude, and g the (mass shell) $\pi N$ coupling constant. This model works well in quantum electrodynamics (possibly because the photon's mass is strictly zero), but the results of this model are too large by at least a factor of ten for $\pi N \to \pi\pi N$.

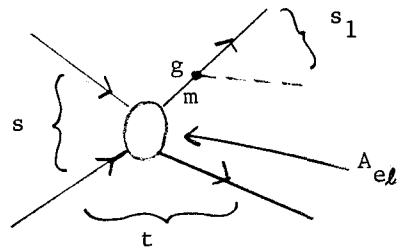


Fig. 35

The main reason for this failure is that the Compton wavelength of the emitted $\pi$ is always smaller than or comparable to the interaction radius.

A more successful model is the "synchrotron radiation model" which is motivated by classical concepts of synchrotron radiation.[34] The power radiated in electrodynamics is proportional to $(\frac{d}{dt}J)^2$. We will consider $pp \to pp\pi$ and assume that in the center of momentum system the protons have classical trajectories that are arcs of circles of radius $\rho$ in the interaction region, which is a sphere of radius R. See Fig. 36. Such a circular trajectory would result if the interaction region contained a uniform magnetic field. The impact parameter $b(\theta)$ is related to $(\frac{d\sigma^{e\ell}}{d\cos\theta})$, $\rho$, and R by the following argument. The elastic cross section is given classically by $d\sigma^{e\ell} = 2\pi b db$. Integrating, we get

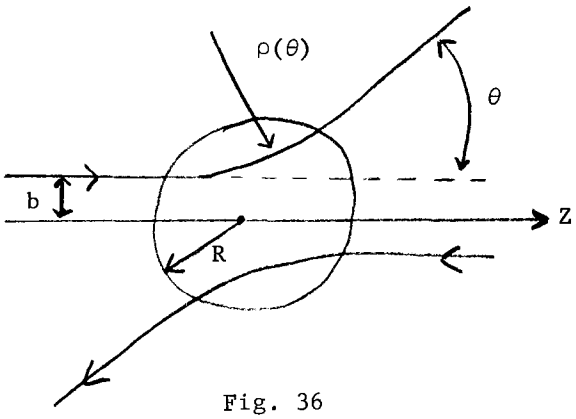


Fig. 36

$$\int_0^b 2\pi b'db' = \int_{\text{backward angle}}^{\cos\theta} \frac{d\sigma^{e\ell}}{d\cos\theta'} d\cos\theta' = \pi b^2(\theta) \quad . \tag{8.1}$$

When $\cos\theta = 1$ we want: $\pi b^2(0) = \pi R^2$ so $b(0) = R$. Geometry gives

$$\rho(\theta) = (R^2-b^2)^{\frac{1}{2}}\cot\frac{\theta}{2} - b(\theta) \quad .$$

Next we assume the particle has a constant velocity so knowing $\rho(\theta)$, we know the trajectory $\vec{r}(t)$.

Next we postulate an appropriate classical current in the form of $J(\vec{x},t) = g\delta(\vec{x}-\vec{r}(t))$ assuming that it is a scalar. The LSZ formalism applied to the amplitude for the diagram in Fig. 37 gives

$$S(k) = < p_1'p_2'k;\text{out}|p_1p_2;\text{in} >$$
$$\sim \int d^4x e^{ik\cdot x} < p_1'p_2';\text{out}|J(x)|p_1p_2;\text{in} > . \tag{8.3}$$

We are assuming that J is a c-number so it can be pulled out of the matrix element leaving

$$S(\vec{k}) \sim < p_1'p_2';\text{out}|p_1p_2\text{in} > \int d^3x e^{i\vec{k}\cdot\vec{x}} \int dt g\delta(\vec{x}-\vec{r}(t)) \tag{8.4}$$

where $< | > = A_{\text{elastic}}(p_1'p_2';p_1p_2)\delta^4(p_1+p_2-p_1'-p_2')$ is taken from data. If the interaction Lagrangian for mesons with nucleons is $g_{\pi N}\phi\psi\gamma_5\psi$, then at large s, -t with $\psi$'s localized in wave packets J is equivalent to $g_{\pi N}\phi\delta(\vec{x}-\vec{r}(t))$ so we get $g=g_{\pi N}$ in this region. Other assumptions are needed, for instance we can take for non-asymptotic t values the replacement

$$A_{\text{elastic}}(s,t) \to (A_{e\ell}(s,t_1)A_{e\ell}(s,t_2))^{\frac{1}{2}} \tag{8.5}$$

to give proper damping in $t_1$ and $t_2$. Also we must symmetrize for the initial protons. Then we can substitute the trajectory $\vec{r}(t)$ in (8.4) and get $S(\vec{k})$. Similar arguments work for vector meson production. There are old data on $pp\to p\pi\pi^+$, $pp\pi^0$, $pp\eta^0$, $pp\omega^0$ at 12.5 GeV which agree fairly well with the model's predictions.[34]

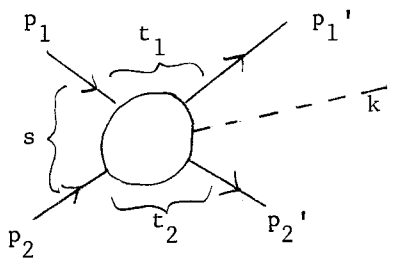


Fig. 37

The synchrotron radiation model works only for large angle production; for small angles we need to assume more quantum properties. We have considered a radiation eikonal model.[35] The main idea is to interpret the interaction

Lagrangian $g\Phi J$ as subtracting probability from elastic scattering. The assumptions are

1) $J = g\frac{d}{dz}|\psi(b,z)|^2$ where $\psi$ is given by (1.7)(one dimensional motion), and

2) $V(b,z) \cong iA\exp[-\frac{b^2}{2R^2} - \frac{\gamma^2 z^2}{2R^2}]$ = the potential occuring in elastic scattering

where $\gamma = E/M$ accounts for Lorentz contraction. The appropriate value of g can be obtained from Adler's self-consistency condition. The S matrix in (8.3) can be generalized to the case of n meson emission if the emissions are assumed to be independent:

$$S(k_1,\ldots,k_n) = \int < p_1' p_2'; \text{out}|p_1 p_2; \text{in} > < j_1(x_1) > \ldots < j_n(x_n) >$$

$$= S_0 \prod_j S_1(k_j) \quad . \tag{8.6}$$

This can be summed to get

$$\sigma_n \sim \int d\Omega_n |S_n|^2 \cong \frac{(g^2)^n}{n!}\Omega_n \cong \frac{(g^2)^n}{n!}(\Omega)^n \tag{8.7}$$

where $\Omega_n$ is a phase space factor. The total inelastic cross section is $\sigma^{\text{inel}} = \sum_n \sigma_n \sim e^{g^2\Omega}$. The probability of producing n particles is

$$\frac{\sigma_n}{\sum_{n'} \sigma_{n'}} \sim \frac{(g^2\Omega)^n}{n!} e^{-g^2\Omega} \quad . \tag{8.8}$$

Maximizing gives $\bar{n} \sim g^2\Omega$ for a Poisson distribution. In Heckman's model,[35]

$$g^2\Omega \equiv \int \frac{d^3k}{\omega}|J(k)|^2 \tag{8.9}$$

increases as $\ell$ns at large s. This model can be used to calculate differential cross sections of $pp \to \pi^+ +$ anything and $pp \to p +$ anything. These are easy to measure with one armed spectrometers and the data have the general features at fixed s shown in Fig. 38. The prediction is in excellent agreement at small angles and starts to differ around angles of $20^\circ$ in the center of momentum system.

Gundzik has worked on a scheme[36] to calculate $pp \to pp$ using the concepts of the above models. In the unitarity diagram in Fig. 39, J is the source and sink of the intermediate pions. The phase of the emitted pions is important here. Also the similar diagram with two N* in the intermediate state is important. Many parameters are needed in this model.

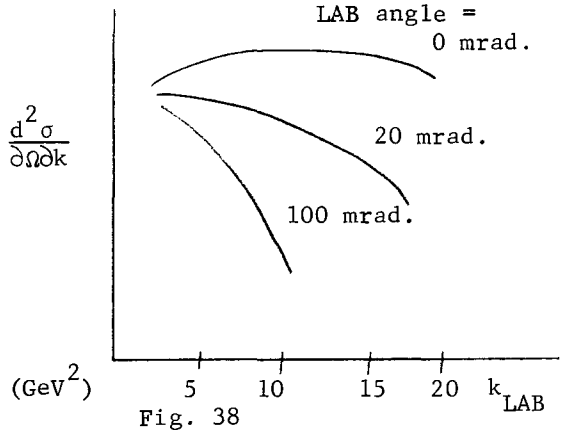

Fig. 38

Another classical theory

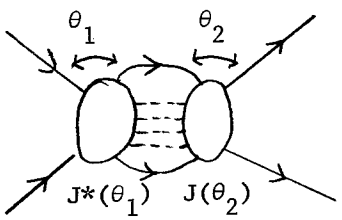


Fig. 39

of multiple production was constructed by Landau ten years ago. It is related to Huang's model since the hadrons are considered to be blobs of gas. When they collide they are assumed to form a symmetrical pill box containing shock waves. The shock wave generates entropy and the flux of entropy is identified with the amount of particles produced.[37] The sequence of events in a collision is illustrated in Fig. 40. The model predicts $n \sim E_{lab}^{\frac{1}{4}}$, which is not contradicted by available data.[38]

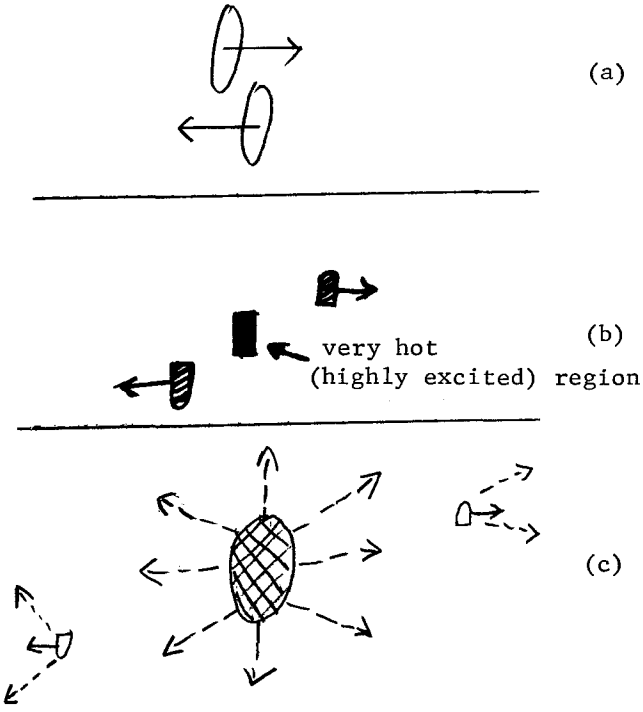


Fig. 40

The number emitted with angle $\theta$ is

$$dn \sim ce^{-\frac{1}{2}((c')^{\frac{1}{2}}-(\eta)^{\frac{1}{2}})^2} d\eta \tag{8.10}$$

where c, c' are constants, depending on the initial state and $\eta = \ell n(\tan\theta)$. The energy flux is given by

$$\omega(\theta) \sim e^{\frac{1}{3}(c''+\eta)-\frac{1}{3}(c''\eta)^{\frac{1}{2}}} . \tag{8.11}$$

Hagedorn's fireball model is similar to the above model in the sense that both have a maximum temperature; however Hagedorn requires arbitrary parameters. Higher energy accelerators are needed to test these models.

In conclusion classically based models work better than diagrammatic models do for the above data. This might be expected since high s is expected to give classical limits. Of course, we may find surprises such as a breakdown of micro-causality; however the operational point of view says try until we find a problem.

## IX. DIELECTRIC SPHERES AND SHARP BOUNDARY MODELS

Consider the scattering of light, of wave number k, by a dielectric sphere of uniform index of refraction n and radius a in optics. Mie solved this fifty years ago. When (k) gets large the solution becomes a sum of many Bessel functions. Nussenzweig[39] used the Sommerfeld-Watson transformation to study this problem. One finds a lot of fine structure as is illustrated in Fig. 41. The shape of $\frac{d\sigma}{d\Omega}$ resembles that of hadron scattering. The peaks occur when $\frac{db}{d\theta} = \infty$. For instance, the backward peak can result from the rays in Fig. 42. The Sommerfeld-Watson transformation for the limit $k \to \infty$ gives J plane singularities (Regge poles) on the locii in Fig. 43. The glory effect is due to poles on the curved section of the locii. The effect can sometimes be observed from an airplane flying over clouds. Sunlight scattered backward from water droplets of the right radius in the clouds can produce bright colored rings around the shadow of the plane. The color implies that the effect is due to a backward diffractive process from small droplets.

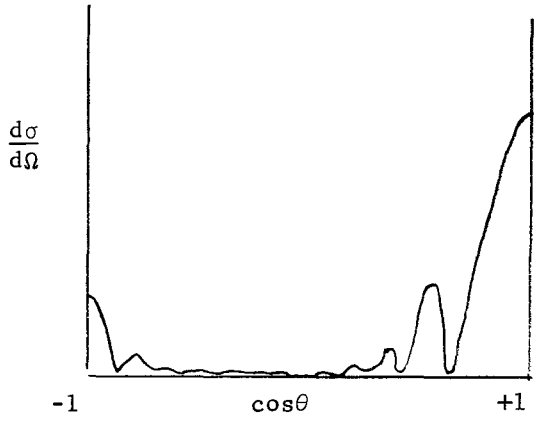


Fig. 41

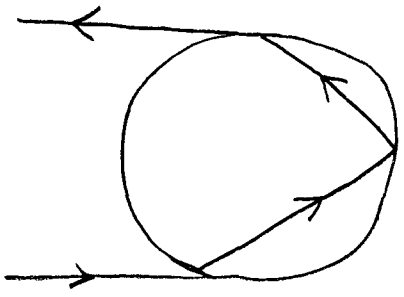

Fig. 42

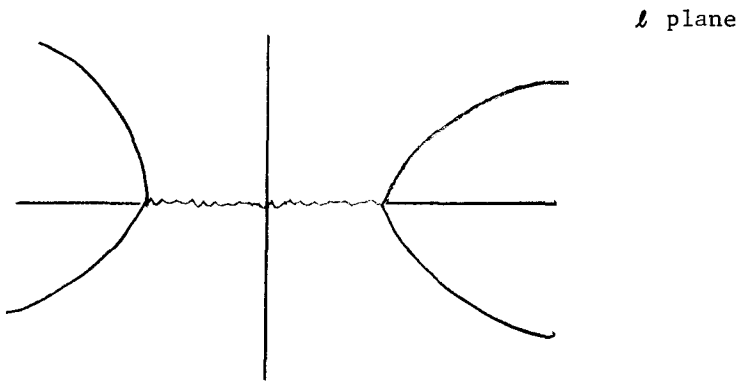


Fig. 43

A quick and dirty derivation of the glory effect from a sharp sphere[40] is the following: write the partial-wave expansion

$$f(\theta) = \frac{1}{2ik} \sum_{\ell} (2\ell+1)(e^{2i\delta_\ell}-1)P_\ell(\cos\theta) \quad . \tag{9.1}$$

Since $P_\ell(-z) = (-)^\ell P_\ell(z)$, (9.1) becomes

$$2ikf(\theta \simeq \pi) \sim \sum_{\ell=0,2,4} (2\ell+1)[e^{2i\delta_\ell}-e^{2i\delta_{\ell+1}}]P_\ell(-\cos\theta). \tag{9.2}$$

If we assume the $e^{2i\delta_\ell}$ is a slowly varying function of $\ell$ then the term in brackets can be approximated by $\frac{\partial}{\partial\ell} e^{2i\delta_\ell}$ and (9.2) becomes

$$f(\theta \simeq \pi) = i\int b\, db J_0(b(-u)^{\frac{1}{2}}) \frac{\partial}{\partial b}[e^{2i\delta(b)}-1] \quad . \tag{9.3}$$

Compare this with the forward amplitude

$$f(\theta \simeq 0) = ik\int b\, db J_0(b(-t)^{\frac{1}{2}})[e^{2i\delta(b)}-1] \quad . \tag{9.4}$$

Thus the backward peak is related to the forward peak. The prediction works roughly for the backward peaks of $\pi^+p$ and $K^+p$ but does not work for $\pi^-p$ and $K^-p$. The s dependence of the peaks is predicted to be

$$\frac{d\sigma}{d\Omega}(\theta \simeq \pi) \simeq \frac{1}{s} \frac{d\sigma}{d\Omega}(\theta \simeq 0) \tag{9.5}$$

which is not strongly violated for such cases. (The assumption that $e^{2\delta_\ell}$ is slowly varying is not good in general.)

A more rigorous approach to the glory effect analogy for backward scattering

is to use the Regge pole expansion. If the Regge poles on the locii in Fig. 43 are assumed to occur at $\alpha(s) = a+bs$ then the backward $\pi p$ peak can be fit.[41] The backward peak in $\pi C$ scattering has been studied in a model where the $\pi$ is internally reflected. $J_0(R(-u)^{\frac{1}{2}})$ fits the data.[42] M.C. Li has been working on similar applications.[43]

The sharpness of the edge of the dielectric sphere is very important in geometrical optics; however, for high s scattering of hadrons, the width of the edge becomes large. If the analogy holds, then the backward peak should go away.[44]

Suppose there is a discontinuity in n in hadrons, for instance, if they are droplets with a skin. Then excited states may be surface waves. For instance, in $pp \to pN^*$ where $N^*$ can be $\frac{1}{2}^+(1480)$, $3/2^-(1520)$, $5/2^+(1690)$, $7/2^-(2190)$, etc., a simple surface-wave model explains the s and t dependence for the first two and fails for the second two.[45] The matrix element to excite $Y_L^M$ surface wave can be approximated by[45]

$$T_L^M(\Delta) = \bar{c}_L Y_L^M(\tfrac{\pi}{2}, 0) \int_0^\infty b db J_M(\Delta b) H(b) \qquad (9.6)$$

where H(b) is the distribution of matter in the interaction region (skin) and $\Delta = (-t)^{\frac{1}{2}}$. For a nearly-square well potential

$$H(b) \sim \frac{\partial}{\partial b}\left(1-e^{i\chi(b)}\right) \quad .$$

We can assume $1-e^{i\chi(b)}$ is a Gaussian in b and then sum the square of (9.6) over M to get the cross section. Perhaps this model is discovering systematics that will come out of someone's dynamics.

## REFERENCES


1. R.J. Glauber, Lectures in Theoretical Physics, Vol. 1, p. 315 (Boulder Colorado Summer School)(1959). A recent review of optical potentials can be found in L.L. Foldy and J.D. Walecka, Ann. Phys. (N.Y.) 54, 447 (1969).
2. R.C. Arnold, Phys. Rev. 153, 1523 (1967). This contains relevant references up to 1966.
3. T.T. Chou and C.N. Yang, Phys. Rev. 170, 1591 (1968).
4. T.T. Chou and C.N. Yang, Rehovoth Conference (1967) p. 348.
5. T.T. Chou and C.N. Yang, Phys. Rev. 175, 1832 (1968).
6. T.T. Chou and C.N. Yang, Phys. Rev. Letters 20, 1213 (1968).
7. J.S. Trefil, Phys. Rev. 180, 1366 and 1379 (1969).
8. C. Wilkin, High Energy Scattering from Nuclei, Nuclear and Particle Physics, McGill University (1967) p. 439.

9. H. Feshbach, Semi-classical Approximation, 37th Course of Enrico Fermi School, (Varenna)(1967).
10. T.T. Wu and C.N. Yang, Phys. Rev. 137, B708 (1965).
11. N. Byers and C.N. Yang, Phys. Rev. 142, 976 (1966).
12. H.M. Chan, Vienna Conference (review talk)(1966).
13. K. Huang, Phys. Rev. 156, 1555 (1967).
14. R. Torgerson, Phys. Rev. 143, 1194 (1966)(Field-Theoretic Eikonal work).
15. A.A. Logunov and A.N. Tavkhelidze, Nuovo Cimento 29, 380 (1963).
16. D.I. Blokhintsev, V.S. Barashenkov and B.M. Barbashov, English Transl: Soviet Physics Uspekhi 2, 505 (1969).
17. H.D.I. Abarbanel and C. Itzykson, Phys. Rev. Letters 23, 53 (1969).
18. H. Cheng and T.T. Wu, Phys. Rev. Letters 22, 666 (1969); 23, 351 (1969).
19. S.J. Chang and S. Ma, Phys. Rev. Letters 22, 1334 (1969).
20. M. Levy and J. Sucher, University of Maryland preprint 983 (1969).
21. C. Chiu and J. Finkelstein, Nuovo Cimento 57, 649 (1968).
22. S. Frautschi and B. Margolis, Nuovo Cimento, 56A, 1155 (1968).
23. S. Frautschi and B. Margolis, Nuovo Cimento 57A, 427 (1968).
24. S. Frautschi and B. Margolis, Nuovo Cimento 61A, 92 (1969).
25. C. Chiu and J. Finkelstein, Nuovo Cimento 57A, 92 (1968).
26. R.C. Arnold and M.L. Blackmon, Phys. Rev. 176, 2082 (1968).
27. M.L. Blackmon and G.R. Goldstein, Phys. Rev. 179, 1480 (1969).
28. S.M. Pruss, C.W. Akerlof, D.I. Meyer, S.P. Ying, J. Lales, R.A. Lundy, D.R. Rust, C.E.W. Ward and D.D. Jovanovitch, Phys. Rev. Letters 23, 189 (1969).
29. S. Mandelstam, Nuovo Cimento 30, 1127 and 1145 (1963).
30. J. Polkinghorne, J. Math. Phys. 6, 1960 (1965).
31. Ya. Azimov et. al., English Transl: Soviet Physics JETP 21, 1189 (1965).
32. L. Caneschi and A. Pignotti, Phys. Rev. Letters 22, 1219 (1969) and L. Caneschi, Phys. Rev. Letters 23, 254 (1969).
33. F. Henyey, G. Kane, J. Pumplin and M. Ross, Phys. Rev. Letters 21, 946 and 1782 (1968); Phys. Rev. 182, 1579 (1969).
34. R.C. Arnold and P. Heckman, Phys. Rev. 164, 1822 (1967).
35. P. Heckman, Ph.D. Thesis, University of Chicago; ANL-HEP
36. M.G. Gundzik, preprint ANL/HEP 6911 (Phys. Rev. to be published).
37. S. Fenster, talk in Argonne Symposium on Multiparticle Production, ANL/HEP 6909.
38. R. Murthy, ibid.
39. H.M. Nussenzweig, J. Math. Phys. 10, 82, 125 (1969).
40. R.C. Arnold, Argonne National Laboratory preprint (1968).
41. H.C. Bryant, SLAC-PUB-608, Stanford preprint (1969).
42. H.C. Bryant and N. Jarmie, Ann. Phys. (N.Y.) 47, 127 (1966).

43. M.C. Li, VPI preprint (1969).

44. E. Montroll and J.M. Greenberg, Phys. Rev. 86, 889 (1952). (They derived the precursor to the eikonal and backward scattering).

45. R.C. Arnold, Phys. Rev. 157, 1292 (1967).